Gadoxetic Acid (Gd-EOB-DTPA)-Enhanced MRI versus Gadobenate Dimeglumine (Gd-BOPTA)-Enhanced MRI for Preoperatively Detecting Hepatocellular Carcinoma: an Initial Experience

Yulri Park, MD[1, 2]
Seong Hyun Kim, MD[1]
Seung Hoon Kim, MD[1]
Yong Hwan Jeon, MD[3]
Jongmee Lee, MD[4]
Min Ju Kim, MD[4]
Dongil Choi, MD[1]
Won Jae Lee, MD[1]
Heejung Kim, MD[1]
Ji Hyun Koo, MD[1]
Hyo Keun Lim, MD[1]

Index terms:
Hepatocellular carcinoma (HCC)
Gadoxetic acid-enhanced MRI
Gadobenate dimeglumine-enhanced MRI

DOI:10.3348/kjr.2010.11.4.433

Korean J Radiol 2010;11:433-440
Received January 8, 2010; accepted after revision April 9, 2010.

[1]Department of Radiology and Center for Imaging Science, Samsung Medical Center, Sungkyunkwan University School of Medicine, Seoul 135-710, Korea; [2]Department of Radiology, Gachon University Gil Hospital, Incheon 405-760, Korea; [3]Department of Radiology, Kangwon National University Hospital, Kangwon-do 200-947, Korea; [4]Department of Radiology, Korea University Guro Hospital, Korea University College of Medicine, Seoul 152-703, Korea

Address reprint requests to:
Seong Hyun Kim, MD, Department of Radiology and Center for Imaging Science, Samsung Medical Center, Sungkyunkwan University School of Medicine, 50 Ilwon-dong, Gangnam-gu, Seoul 135-710, Korea.
Tel. (822) 3410-0511
Fax. (822) 3410-0084
e-mail: kshyun@skku.edu

Objective: This study was designed to compare the diagnostic performance of gadoxetic acid-enhanced magnetic resonance imaging (MRI) with gadobenate dimeglumine-enhanced MRI for preoperatively detecting hepatocellular carcinoma (HCC).

Materials and Methods: Eighteen consecutive patients (17 men and one woman, age range: 31–73 years) with 22 HCCs underwent examinations with gadoxetic acid enhanced MRI and gadobenate dimeglumine-enhanced MRI on a 3.0-Tesla unit. The diagnosis of HCC was established after surgical resection and pathological conformation. Three observers independently reviewed each MR image in a random order on a tumor-by-tumor basis. The diagnostic accuracy of these techniques for the detection of HCC was assessed by performing an alternative free-response receiver operating characteristic (ROC) analysis. The sensitivity and positive predictive values were evaluated.

Results: The average value of the area under the ROC curve (Az) for gadoxetic acid enhanced MRI (0.887) was not significantly different from the Az (0.899) for gadobenate dimeglumine-enhanced MRI ($p > 0.05$). The overall sensitivities of gadoxetic acid enhanced MRI and gadobenate dimeglumine-enhanced MRI were 80% and 83%, respectively, with no significant difference ($p > 0.05$). The differences of the positive predictive values for the two contrast agents for each observer were not statistically significant ($p > 0.05$).

Conclusion: The diagnostic performance of gadoxetic acid-enhanced MRI and gadobenate dimeglumine-enhanced MRI for preoperatively detecting HCC is quite similar.

Various liver contrast agents for magnetic resonance imaging (MRI) have been developed to characterize focal hepatic lesions. Among these agents, gadolinium-based hepatobiliary agents are advantageous to utilize for the detection as well as the characterization of hepatic focal lesions. Two gadolinium-based hepatobiliary agents have been clinically approved and are now being used: gadolinium ethoxybenzyl diethylenetriaminepentaacetic acid (gadoxetic acid disodium or Gd-EOB-DTPA; Primovist, Schering, Berlin, Germany) and gadobenate dimeglumine (Gd-BOPTA/Dimeg, Multihance, Bracco, Milano, Italy). Both agents are distributed in the extracellular-interstitial space immediately after intravenous administration. Subsequently, the agents are taken up by functional hepatocytes, which is a process mediated by organic anion transporter, and the compounds are excreted into the bile (1–6). The biliary excretion rate of gadobenate dimeglumine is

approximately 3–5%, whereas the biliary excretion rate of gadoxetic acid is up to 50% (1, 3–5, 7, 8). In addition, gadoxetic acid has an advantage in terms of obtaining its hepatobiliary phase as early as 20 min following contrast injection, while gadobenate dimeglumine-enhanced MRI is performed > 60 min following injection (9, 10).

For the detection of hepatocellular carcinoma (HCC) in patients with chronic liver disease, gadobenate dimeglumine-enhanced MRI has demonstrated a higher sensitivity than has multidetector CT (MDCT) for HCCs ($\leq$ 1 cm) (11) and gadobenate dimeglumine-enhanced MRI has demonstrated a better diagnostic performance than ferucarbotran-enhanced MRI (12). However, to the best of our knowledge, there have been no studies that have compared gadoxetic acid-enhanced MRI and gadobenate dimeglumine-enhanced MRI with a 3.0 Tesla unit for the detection of HCC. The purpose of this study was to evaluate and compare the diagnostic performance of these two MRI methods for preoperatively detecting HCC.

MATERIALS AND METHODS

Study Population

This is a retrospective study. Between January 2007 and January 2008, 65 consecutive patients who were suspected of having HCCs based on a sonographic evaluation and the presence of an elevated level of α-fetoprotein underwent gadobenate dimeglumine-enhanced MRI at our institution. Among these patients, 30 patients also underwent gadoxetic acid-enhanced MRI. For all the patients, gadoxetic acid-enhanced MRI was performed at an interval of five to 29 days after performing gadobenate dimeglumine-enhanced MRI. Of the 30 patients who also underwent gadoxetic acid-enhanced MRI, 18 patients (17 men and one woman, age range: 31–73 years, mean age: 53.3 years) underwent hepatic surgery with identifying 22 pathologically proven HCCs and these 18 patients were eventually enrolled in this study. Of these 18 patents, a portion of these patients, who were enrolled in a previous report (13), were included because this study's retrospective study design. All the hepatic surgeries were performed within five days from the last pre-operative gadoxetic acid enhanced MRI. Seven patients underwent segmentectomy, six patients underwent bisegmentectomy and five patients underwent right lobectomy. The 22 HCCs ranged from 0.5 cm to 10.0 cm in diameter (two HCCs were < 1 cm in diameter, six HCCs were 1 cm $\leq$ diameter < 2 cm, and 14 HCCS were $\geq$ 2 cm in diameter, mean diameter, 2.9 cm). The histological grades of the tumors included two well-differentiated HCCs, 17 moderately differentiated HCCs and three poorly-differentiated HCCs. Twelve patients (11 patients with hepatitis B virus and one with hepatitis C virus) had cirrhosis, five patients had chronic B virus related hepatitis and one patient had a normal liver. Written informed consent for the liver MRI examinations were obtained from all the patients. Approval by the Institutional Review Board was waived because this was a retrospective study.

MR Imaging

MRI examinations were performed with a 3.0 Tesla whole-body MR system (Intera Achieva 3.0T; Philips Medical Systems, Best, The Netherlands) with a 6-channel phased-array coil as the receiver coil. The MRI protocols and sequences were as follows: a respiratory triggered T1-weighted turbo-field-echo in-phase sequence (TR/TE: 10 ms/2.3 ms, flip angle: 15°, matrix: 288 × 230, bandwidth: 434.3 Hz per pixel), an out-of-phase sequence (TR/TE: 10 ms/3.45 ms, flip angle: 15°, matrix: 288 × 230, bandwidth: 434.3 Hz per pixel), a respiratory-triggered single-shot T2-weighted sequence with a reduction factor of two or four (TR/TE: 1,342 ms/80 ms, flip angle: 90°, matrix: 320 × 256, bandwidth: 506.4 Hz per pixel), a breath-hold multi-shot T2-weighted sequence with a reduction factor of two or four (TR/TE: 2,161 ms/70 ms, flip angle: 90°, matrix: 400 × 280, bandwidth: 235.2 Hz per pixel), a respiratory-triggered single-shot heavily T2-weighted sequence with a reduction factor of two or four (TR/TE: 1,573 ms/160 ms, flip angle: 90°, matrix: 320 × 256, bandwidth: 317.9 Hz per pixel) with a 5–7 mm section thickness, a 1-mm to 2-mm intersection gap and a field of view of 32–38 cm. A dose of 0.1 mL/kg (0.025 mmol/kg gadoxetic acid; 0.05 mmol/kg gadobenate dimeglumine) contrast agent was manually administered intravenously at a rate of 2 mL/sec, followed by a 20 mL saline solution flush. For the contrast-enhanced MRI, the unenhanced, arterial phase (20–35 sec), portal phase (70 sec), equilibrium phase (3 min) and hepatobiliary phase sequences were obtained using T1-weighted three-dimensional turbo-field-echo imaging (T1 high resolution isotropic volume examination; THRIVE, Philips Medical Systems, Best, The Netherlands) (TR/TE: 3.4 ms/1.8 ms, flip angle: 10°, matrix: 336 × 206, bandwidth: 995.7 Hz per pixel) with a 2 mm section thickness with no intersection gap and a field of view of 32–38 cm. The hepatobiliary phase images were obtained 20 minutes after the administration of gadoxetic acid. For gadobenate dimeglumine, the hepatobiliary phase images were obtained three hours after the administration to minimize its extracellular effect.

Image Analysis

Three radiologists who each had at least two years experience with interpreting MR images reviewed all of the MR images on a 2,000 × 2,000 picture archiving and communications system (PACS; PathSpeed workstation; GE Healthcare, Milwaukee, WI) workstation in a random order and in a blinded fashion. They were unaware which contrast agent was used when reading the images. The interval between the reviews of the two MRI examinations was at least one month. Each observer recorded the presence and segment location of the HCC lesions by using a four-point scale to assign a confidence level to each lesion. The scores were 1: probably not an HCC lesion, 2: a possible HCC lesion, 3: a probable HCC lesion and 4: a definite HCC lesion. An HCC was defined as showing typical arterial enhancement and venous washout irrespective of its size, based on previous studies (14–19). Nodules larger than 2 cm with predominant hypointensity, as seen on the contrast-enhanced portal and equilibrium phases with no definite arterial enhancement, were also regarded as HCCs (19, 20). In addition to these features, a hypointense nodule seen on the hepatobiliary phase MR images was considered as an HCC based on the findings of a previous report (21). A hypervascular nodule seen on the contrast-enhanced arterial phase with a washout pattern was considered as an HCC, although the nodule was seen with isointensity or hyperintensity relative to the surrounding liver parenchyma on the hepatobiliary phase (21, 22). To achieve accurate correlation between the findings of the scored lesions and the reference standard, each observer recorded the individual image number, the locations of all of the lesions and the diameter of each lesion. For patients with multiple lesions located in the same segment, the observers added further descriptions regarding the size and location of the lesion within each segment in order to avoid confusion during the data analysis. The sensitivities were calculated using the number of lesions assigned a confidence level of 3 or 4. All false-positive findings with confidence levels of 3 or 4 and that were confirmed as benign lesions, or all false-negative findings with confidence levels of 1 or 2 and that were confirmed as an HCC, were assessed by two study coordinators who worked in consensus.

For the quantitative analysis, a radiologist chose the regions of interest on the MR images. For heterogeneous lesions, the regions of interest were chosen in the more homogeneous areas. Areas of intratumoral necrosis or hemorrhage were excluded from the regions of interest. Measurements of tumors and the background along the phase-encoding axis were obtained from the same areas on the six images. The contrast-to-noise ratios (CNRs) were calculated using (SIL-SIBL)/SDN, where SIL is the signal intensity (SI) of the lesion, SDN is the standard deviation of the background noise and SIBL is the mean SI of the background liver. For measurement purposes, 17 tumors that were 1 cm or more in diameter and visible on the images obtained with all the pulse sequences were chosen for the analysis in order to reduce any measurement inaccuracies resulting from partial volume effects.

Statistical Analysis

On the basis of the three observers' reviews, an alternative free-response receiver operating characteristic (ROC) curve was generated on a tumor-by-tumor basis. The diagnostic performance of each contrast agent for each observer was assessed by measuring the area under the ROC curve (Az), in accordance with a previous report (23), and the average Az values for the two contrast agents were compared as previously described by McNeil et al. (24).

The sensitivity for each observer and technique was calculated and the differences of the sensitivities were assessed by the McNemar test. Statistical analysis for the overall sensitivities of the two techniques for all observers was assessed by the generalized estimating equation. Statistical analyses for the differences of the calculated positive predictive values for each observer and technique were based on a previous study (25). A p value less than 0.05 was considered to indicate a statistically significant difference. An analysis of all false-positive and false-negative observations was also undertaken. Kappa statistics were used to assess the interobserver agreement for the detection of HCCs with the use of each technique. The degree of agreement was categorized as follows: kappa values of 0.00–0.20 were considered to indicate poor agreement, kappa values of 0.21–0.40 indicated fair agreement, kappa values of 0.41–0.60 indicated moderate agreement, kappa values of 0.61–0.80 indicated good agreement and kappa values of 0.81–1.00 indicated excellent agreement (26).

In the quantitative image analysis, the tumor to liver CNR of each phase was statistically compared using the Wilcoxon signed ranks test.

RESULTS

For all 22 HCCs evaluated, the calculated Az values for each observer for the gadoxetic acid- and gadobenate dimeglumine-enhanced MRI are shown in Table 1. All the observers achieved similar diagnostic accuracy with the two techniques (Fig. 1); the average Az values obtained for the use of gadoxetic acid (0.887) and gadobenate dimeglu-

Table 1. Area Under Receiver Operating Curve (Az) for Gadoxetic Acid-Enhanced MRI and Gadobenate Dimeglumine-Enhanced MRI for Detecting 22 Hepatocellular Carcinomas

Technique	Observer 1	Observer 2	Observer 3	Average
Gadoxetic acid-enhanced MRI	0.903	0.864	0.894	0.887
Gadobenate dimeglumine-enhanced MRI	0.942	0.870	0.886	0.899
Difference in Az	0.039	0.007	0.008	0.012
P	0.293	0.782	0.865	0.780

Note.— Data are given as Az values.

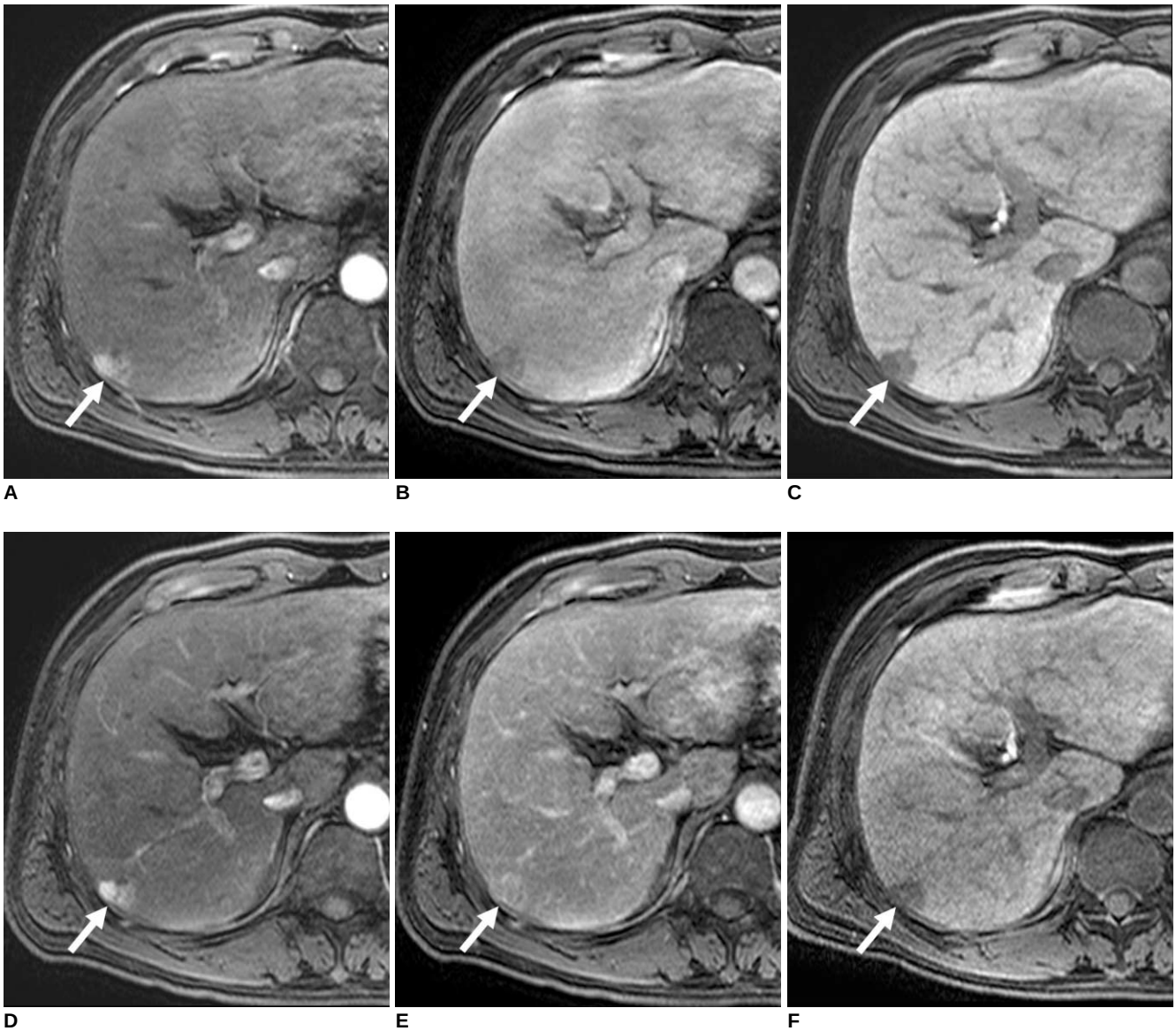

Fig. 1. 50-year-old man with 1.8 cm moderately differentiated hepatocellular carcinoma (arrows) in liver segment VI.
A-C. Gadoxetic acid-enhanced transverse MR images show arterial enhancement (**A**), washout during equilibrium phase (**B**) and hypointensity during hepatobiliary phase (**C**). This lesion was detected by all of observers. Tumor-to-liver contrast-to-noise ratios were 15, −2.1 and −30.1 during arterial, equilibrium and hepatobiliary phases, respectively.
D-F. Gadobenate dimeglumine-enhanced transverse MR images show arterial enhancement (**D**), no washout during equilibrium phase (**E**) and hypointensity during hepatobiliary phase (**F**). This lesion was detected by all of observers. Tumor-to-liver contrast-to-noise ratios were 36.7, 9.8 and −4.9, during arterial, equilibrium and hepatobiliary phases, respectively.

mine enhanced MRI (0.899) for all the observers were not significantly different ($p = 0.780$).

The sensitivities for each observer and each MRI examination were calculated (Table 2). The difference in the overall sensitivities of the two techniques for all the observers was not statistically significant ($p = 0.317$). None of the observers showed statistically significant differences for the positive predictive values between the two techniques ($p > 0.05$) (Table 2).

Gadoxetic acid-enhanced MRI resulted in identifying five false positive lesions, and gadobenate dimeglumine-enhanced MRI resulted in identifying seven false positive lesions. Four lesions (80%) depicted on the gadoxetic acid-enhanced MRI and five lesions (71%) depicted on the gadobenate dimeglumine-enhanced MRI were identified as arterioportal shunts. All nine lesions that were misinterpreted by the three observers were the same three arterioportal shunts. One necrotic cirrhosis-related nodule was misinterpreted as an HCC with both techniques. Another necrotic cirrhosis-related nodule was misinterpreted as an HCC only on the gadobenate dimeglumine-enhanced MRI.

Gadoxetic acid-enhanced MRI depicted 13 false negative lesions and gadobenate dimeglumine-enhanced MRI depicted 11 false negative lesions. Three HCCs were not detected using the two techniques by all the observers. The sizes and histological grades of these three tumors were a 0.5 cm poorly-differentiated tumor, a 0.6 cm moderately-differentiated tumor and a 1.3 cm well-differentiated tumor. Based on a retrospective analysis, the 0.5 cm HCC could not be seen on any images and the 0.6 cm HCC was missed due to an error by the observers on a retrospective review (Fig. 2). The well differentiated 1.3 cm HCC was seen with isointensity relative to the surrounding liver on the hepatobiliary phase images, with no hypervascularity on the arterial phase and with hypointensity only on the equilibrium phase of both MRI methods, which resulted in the false-negative result in the retrospective analysis.

One moderately-differentiated HCC that was 1.1 cm in the right liver dome was detected only on the gadobenate dimeglumine-enhanced MR images by the two observers, and it was not depicted on the gadoxetic acid-enhanced MR images by any of the observers.

There was no HCC was detected only on the gadoxetic acid-enhanced MR images and not on the gadobenate

Table 2. Sensitivities and Positive Predictive Values of Gadoxetic Acid-Enhanced MRI and Gadobenate Dimeglumine-Enhanced MRI for Detecting 22 Hepatocellular Carcinomas

Technique	Observer 1	Observer 2	Observer 3	Overall
Sensitivity per Lesion (%)[a]				
Gadoxetic acid-enhanced MRI	81.8 (18)	77.3 (17)	81.8 (18)	80.3 (53)
Gadobenate dimeglumine-enhanced MRI	86.4 (19)	81.8 (18)	81.8 (18)	83.3 (55)
Positive Predictive Value (%)[b]				
Gadoxetic acid-enhanced MRI	94.7 (18/19)	85.0 (17/20)	94.7 (18/19)	
Gadobenate dimeglumine-enhanced MRI	90.5 (19/21)	94.7 (18/19)	81.8 (18/22)	

Note.— [a]Data in parentheses are number of true-positive lesions. [b]Data in parentheses are number of true-positive lesions divided by total number of lesions assigned confidence level of 3 or 4. Differences of sensitivities and positive predictive values for two techniques for each observer are not statistically significant ($p > 0.05$).

Table 3. Interobserver Agreement Regarding Presence of Hepatocellular Carcinoma

Technique	Observer 1 versus Observer 2	Observer 2 versus Observer 3	Observer 1 versus Observer 3
Gadoxetic acid-enhanced MRI	0.856	0.761	0.904
Gadobenate dimeglumine-enhanced MRI	0.951	0.668	0.768

Note.— Data are shown as kappa values.

Table 4. Contrast-to-Noise Ratio Patterns of 17 Hepatocellular Carcinomas over 1 cm

Technique	AP	PP	EP	HBP
Gadoxetic acid-enhanced MRI	−8.7~21 (4.0)	−9.9~13.4 (−1.8)	−16.2~5.6 (−6.8)	−34.4~−3.4 (−16.1)
Gadobenate dimeglumine-enhanced MRI	−13.8~36.7 (7.3)	−11.1~14.7 (−0.4)	−12.7~16.1 (0.7)	−25.5~−0.8 (−8.3)
P	0.309	0.492	0.478	0.000

Note.— Data shown are range of contrast-to-noise ratios and data in parentheses are mean of contrast-to-noise ratio.
AP = arterial phase, EP = equilibrium phase, HBP = hepatobiliary phase, PP = portal phase

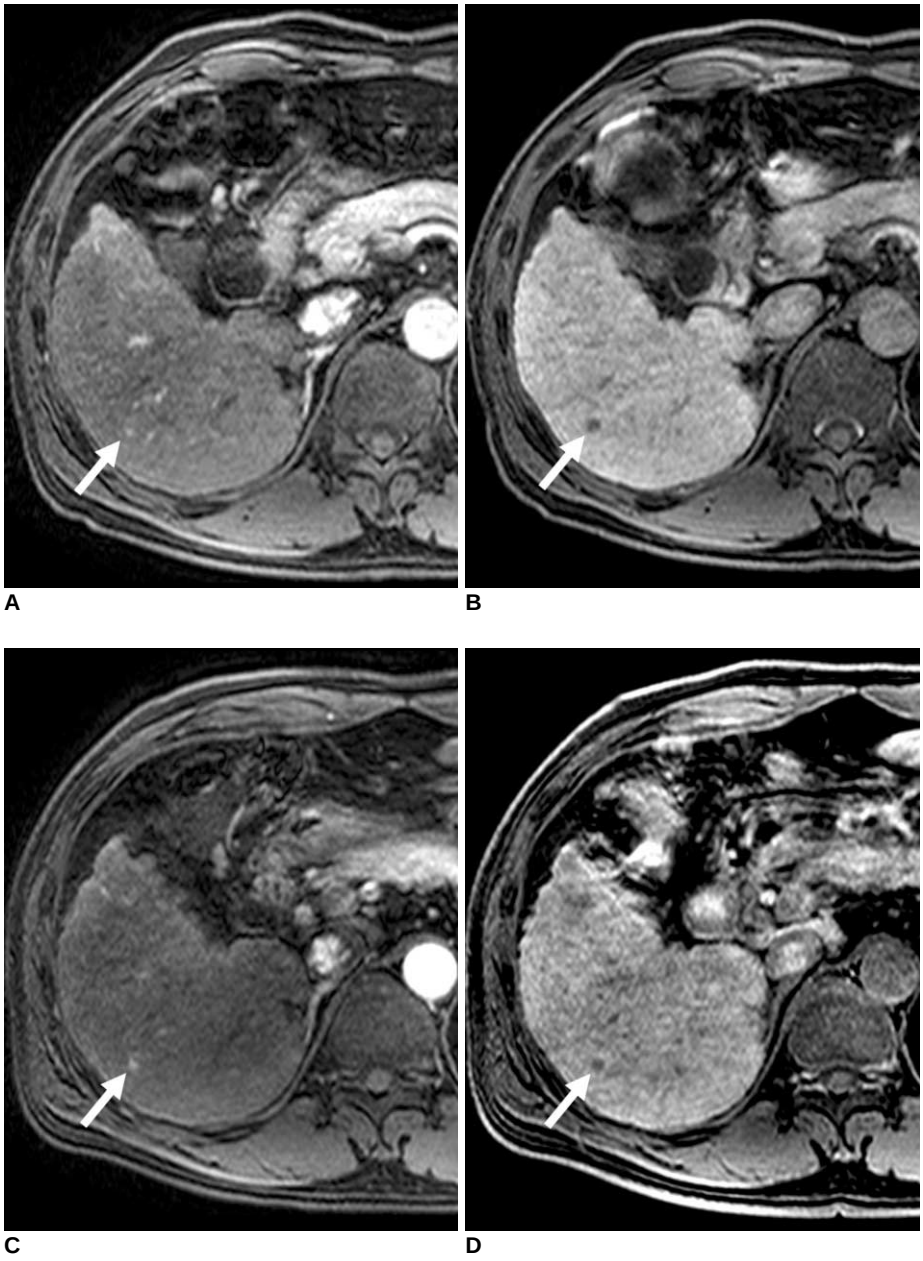

Fig. 2. 47-year-old man with 0.6 cm moderate-differentiated hepatocellular carcinoma (arrows) in liver segment VI. **A, B.** Gadoxetic acid-enhanced transverse MR images show arterial enhancement (**A**), washout during equilibrium phase (not shown) and hypointensity during hepatobiliary phase (**B**). All of observers missed this lesion. **C, D.** Gadobenate dimeglumine-enhanced transverse MR images show arterial enhancement (**C**), washout during equilibrium phase (not shown) and hypointensity during hepatobiliary phase (**D**). All of observers missed this lesion.

dimeglumine-enhanced MR images. The kappa values among the three observers showed good and excellent agreement for the two techniques (Table 3).

Table 4 showed the range of the CNRs of 17 HCCs during the four phases, respectively. All the tumors had the maximum absolute CNR during the arterial or hepatobiliary phase. The differences of the CNR during each of the four phases were statistically significant only during the hepatobiliary phase (Fig. 1).

DISCUSSION

High-field-strength MRI and the development of techniques such as parallel imaging has resulted in an increase of the signal-to-noise ratio, reduction of motion artifacts and better conditions that minimize the scan time and improve MR imaging (27–30). In addition to the MRI techniques, the development of hepatic contrast agents is a major factor for achieving better diagnostic accuracy of hepatic focal lesions. Gadoxetic acid, which has recently been used in clinical practice, is the second gadolinium-based hepatobiliary agent developed for clinical use and it is advantageous as the hepatobiliary phase can be obtained at 10 or 20 minutes post-injection, as compared with that of gadobenate dimeglumine for which the hepatobiliary phase can be obtained at 1–3 hours post-injection. Gadoxetic acid also has a potential merit, due to its high rate of biliary excretion, for use in patients who are at risk

of nephrogenic systemic sclerosis. Since the biliary excretion rate of gadoxetic acid is superior to that of gadobenate dimeglumine, we thought that the strong enhancement of the liver parenchyma and the high CNR during the hepatobiliary phase of gadoxetic acid-enhanced MRI might result in improved diagnostic accuracy for detecting HCCs and this would be similar as that of gadobenate dimeglumine-enhanced MRI.

On our quantitative analysis, there was a significant difference of CNRs during hepatobiliary phase, and this difference is based on the higher bile excretion rate of gadoxetic acid than that of gadobenate dimeglumine. Yet the two imaging techniques had similar diagnostic accuracy, sensitivity and positive predictive values. One possible reason for this is that the precontrast scans and dynamic imaging to assess the hemodynamics of the lesions were similar for both contrast agents. Second, although the estimated relaxivity of gadoxetic acid is 16.6 mmol-1s-1 and this is lower than that of gadobenate dimeglumine (6), the earlier and rapider biliary excretion of gadoxetic acid may compensate for this disadvantage and improve the CNR during the hepatobiliary phase, which helped to obtain comparable results using both contrast agents.

In our study, the majority of false positive lesions on both the gadoxetic acid-enhanced MRI (80%) and the gadobenate dimeglumine-enhanced MRI (71%) were primarily attributed to an arterioportal shunt. We believe that an arterioportal shunt is an important mimicker of HCC that causes difficulty to differentiate small HCCs on both the gadoxetic acid- and gadobenate dimeglumine-enhanced dynamic MR images. On the retrospective review, all of the arterioportal shunts showed no hypointensity on the hepatobiliary phase images, which may be helpful for differentiating these lesions from small HCCs. In a recent study, most of the arterial-enhancing pseudo lesions showed isointensity during the hepatobiliary phase and a few lesions showed hypointensity on the gadoxetic acid-enhanced MRI (31).

There were three false negative lesions for both contrast agents by all the observers. Two of them were too small to detect. One was due to the detection error and the other was due to no delineation even though the images of both MRI examinations were retrospectively reviewed. The remaining false negative lesion, a 1.3 cm HCC, was seen with isointensity on the unenhanced, arterial and hepatobiliary images, but this lesion was seen with hypointensity only on the equilibrium phase for both MRI contrast agents. All of the observers misinterpreted the lesion as a benign cirrhosis-related nodule because of the atypical enhancement. We think that one possible reason observers misinterpret or miss HCCs in clinical practice may be due to the hyper- or isointensity of HCCs during the hepatobiliary phase of MRI with using both contrast agents. Therefore, one should be aware that HCC cannot be completely ruled out when HCC tumors in patients with chronic liver disease show iso- or hyperintensity on the hepatobiliary phase images, as several investigators have reported the paradoxical uptake of gadoxetic acid or gadobenate dimeglumine in HCC (21, 32). Another possible reason is that small HCC and well differentiated HCC can have the atypical enhancement, such as the lack of arterial hypervascularity (33).

One 1.1 cm HCC was interpreted correctly only on the gadobenate dimeglumine enhanced MRI by two observers. As seen on the gadobenate dimeglumine-enhanced MR images, the presence of arterial nodular enhancement allowed making an exact diagnosis in spite of the presence of isointensity seen on the unenhanced and equilibrium phase images and the hyperintensity seen on the hepatobiliary images, while arterial hypervascularity was not found on the gadoxetic acid-enhanced MR images. We can speculate that in addition to the technical errors due to the location of the tumor in the liver dome, a lesser concentration of gadoxetic acid, as compared to that of gadobenate dimeglumine, may lead to the loss of arterial hypervascularity on the gadoxetic acid-enhanced MR images.

This study has some limitations. First, the enrolled population was not sufficient to completely verify the diagnostic performance, and the small population may have led to the detection of a small number of false positive lesions. Second, the study group was limited to patients with good hepatic function and so they could undergo hepatic resection, and this limitation might have caused a selection bias that may have resulted in a higher diagnostic performance.

In conclusion, gadoxetic acid-enhanced MRI and gadobenate dimeglumine-enhanced MRI have similar diagnostic performances for preoperatively detecting HCCs in patients with chronic liver disease.

References

1. Schuhmann-Giampieri G, Schmitt-Willich H, Press WR, Negishi C, Weinmann HJ, Speck U. Preclinical evaluation of Gd-EOB-DTPA as a contrast agent in MR imaging of the hepatobiliary system. *Radiology* 1992;183:59-64
2. van Montfoort JE, Stieger B, Meijer DK, Weinmann HJ, Meier PJ, Fattinger KE. Hepatic uptake of the magnetic resonance imaging contrast agent gadoxetate by the organic anion transporting polypeptide Oatp 1. *J Pharmacol Exp Ther* 1999;290:153-157
3. de Haen C, Gozzini L. Soluble-type hepatobiliary contrast agents for MR imaging. *J Magn Reson Imaging* 1993;3:179-186
4. Kirchin MA, Pirovano GP, Spinazzi A. Gadobenate dimeglumine (Gd-BOPTA). An overview. *Invest Radiol* 1998;33:798-

809
5. Spinazzi A, Lorusso V, Pirovano G, Kirchin M. Safety, tolerance, biodistribution, and MR imaging enhancement of the liver with gadobenate dimeglumine: results of clinical pharmacologic and pilot imaging studies in nonpatient and patient volunteers. *Acad Radiol* 1999;6:282-291
6. Schuhmann-Giampieri G. Liver contrast media for magnetic resonance imaging. Interrelations between pharmacokinetics and imaging. *Invest Radiol* 1993;28:753-761
7. Spinazzi A, Lorusso V, Pirovano G, Taroni P, Kirchin M, Davies A. Multihance clinical pharmacology: biodistribution and MR enhancement of the liver. *Acad Radiol* 1998;5:S86-S89
8. Hamm B, Staks T, Muhler A, Bollow M, Taupitz M, Frenzel T, et al. Phase I clinical evaluation of Gd-EOB-DTPA as a hepatobiliary MR contrast agent: safety, pharmacokinetics, and MR imaging. *Radiology* 1995;195:785-792
9. Reimer P, Schneider G, Schima W. Hepatobiliary contrast agents for contrast-enhanced MRI of the liver: properties, clinical development and applications. *Eur Radiol* 2004;14:559-578
10. Hwang HS, Kim SH, Jeon TY, Choi D, Lee WJ, Lim HK. Hypointense hepatic lesions depicted on gadobenate dimeglumine-enhanced three-hour delayed hepatobiliary-phase MR imaging: differentiation between benignancy and malignancy. *Korean J Radiol* 2009;10:294-302
11. Kim YK, Kim CS, Chung GH, Han YM, Lee SY, Chon SB, et al. Comparison of gadobenate dimeglumine-enhanced dynamic MRI and 16-MDCT for the detection of hepatocellular carcinoma. *AJR Am J Roentgenol* 2006;186:149-157
12. Kim YK, Kim CS, Lee YH, Kwak HS, Lee JM. Comparison of superparamagnetic iron oxide-enhanced and gadobenate dimeglumine-enhanced dynamic MRI for detection of small hepatocellular carcinomas. *AJR Am J Roentgenol* 2004;182:1217-1223
13. Kim SH, Kim SH, Lee J, Kim MJ, Jeon YH, Park Y, et al. Gadoxetic acid-enhanced MRI versus triple-phase MDCT for the preoperative detection of hepatocellular carcinoma. *AJR Am J Roentgenol* 2009;192:1675-1681
14. Baron RL, Oliver JH, 3rd, Dodd GD, 3rd, Nalesnik M, Holbert BL, Carr B. Hepatocellular carcinoma: evaluation with biphasic, contrast-enhanced, helical CT. *Radiology* 1996;199:505-511
15. Bruix J, Sherman M; Practice Guidelines Committee, American Association for the Study of Liver Diseases. Management of hepatocellular carcinoma. *Hepatology* 2005;42:1208-1236
16. Bruix J, Sherman M, Llovet JM, Beaugrand M, Lencioni R, Burroughs AK, et al. Clinical management of hepatocellular carcinoma. Conclusions of the Barcelona-2000 EASL Conference. European Association for the Study of the Liver. *J Hepatol* 2001;35:421-430
17. Jang HJ, Lim JH, Lee SJ, Park CK, Park HS, Do YS. Hepatocellular carcinoma: are combined CT during arterial portography and CT hepatic arteriography in addition to triple-phase helical CT all necessary for preoperative evaluation? *Radiology* 2000;215:373-380
18. Kang BK, Lim JH, Kim SH, Choi D, Lim HK, Lee WJ, et al. Preoperative depiction of hepatocellular carcinoma: ferumoxides-enhanced MR imaging versus triple-phase helical CT. *Radiology* 2003;226:79-85
19. Sherman M. Diagnosis of small hepatocellular carcinoma. *Hepatology* 2005;42:14-16
20. Bolondi L, Gaiani S, Celli N, Golfieri R, Grigioni WF, Leoni S, et al. Characterization of small nodules in cirrhosis by assessment of vascularity: the problem of hypovascular hepatocellular carcinoma. *Hepatology* 2005;42:27-34
21. Huppertz A, Haraida S, Kraus A, Zech CJ, Scheidler J, Breuer J, et al. Enhancement of focal liver lesions at gadoxetic acid-enhanced MR imaging: correlation with histopathologic findings and spiral CT--initial observations. *Radiology* 2005;234:468-478
22. Narita M, Hatano E, Arizono S, Miyagawa-Hayashino A, Isoda H, Kitamura K, et al. Expression of OATP1B3 determines uptake of Gd-EOB-DTPA in hepatocellular carcinoma. *J Gastroenterol* 2009;44:793-798
23. Hanley JA, McNeil BJ. A method of comparing the areas under receiver operating characteristic curves derived from the same cases. *Radiology* 1983;148:839-843
24. McNeil BJ, Hanley JA, Funkenstein HH, Wallman J. Paired receiver operating characteristic curves and the effect of history on radiographic interpretation. CT of the head as a case study. *Radiology* 1983;149:75-77
25. Bennett BM. On comparisons of sensitivity, specificity and predictive value of a number of diagnostic procedures. *Biometrics* 1972;28:793-800
26. Fleiss JL. *The measurement of interrater agreement*. In: Fleiss JL, ed. *Statistical methods for the rates and proportions*, 2nd ed. New York, NY: John Wiley & Sons, 1981:212-236
27. Uematsu H, Takahashi M, Dougherty L, Hatabu H. High field body MR imaging: preliminary experiences. *Clin Imaging* 2004;28:159-162
28. Lüdeke KM, Röschmann P, Tischler R. Susceptibility artefacts in NMR imaging. *Magn Reson Imaging* 1985;3:329-343
29. Kurihara Y, Yakushiji YK, Tani I, Nakajima Y, Van Cauteren M. Coil sensitivity encoding in MR imaging: advantages and disadvantages in clinical practice. *AJR Am J Roentgenol* 2002;178:1087-1091
30. Chang JM, Lee JM, Lee MW, Choi JY, Kim SH, Lee JY, et al. Superparamagnetic iron oxide-enhanced liver magnetic resonance imaging: comparison of 1.5 T and 3.0 T imaging for detection of focal malignant liver lesions. *Invest Radiol* 2006;41:168-174
31. Sun HY, Lee JM, Shin CI, Lee DH, Moon SK, Kim KW, et al. Gadoxetic acid-enhanced magnetic resonance imaging for differentiating small hepatocellular carcinomas (< or = 2 cm in diameter) from arterial enhancing pseudolesions: special emphasis on hepatobiliary phase imaging. *Invest Radiol* 2010;45:96-103
32. Kim JI, Lee JM, Choi JY, Kim YK, Kim SH, Lee JY, et al. The value of gadobenate dimeglumine-enhanced delayed phase MR imaging for characterization of hepatocellular nodules in the cirrhotic liver. *Invest Radiol* 2008;43:202-210
33. Yoon SH, Lee JM, So YH, Hong SH, Kim SJ, Han JK, et al. Multiphasic MDCT enhancement pattern of hepatocellular carcinoma smaller than 3 cm in diameter: tumor size and cellular differentiation. *AJR Am J Roentgenol* 2009;193:W482-W489